Biochemical and Biophysical Research Communications 437 (2013) 609–614

Contents lists available at SciVerse ScienceDirect

Biochemical and Biophysical Research Communications

journal homepage: www.elsevier.com/locate/ybbrc

Cathelicidin antimicrobial peptide inhibits fibroblast migration via P2X7 receptor signaling

Shohei Kumagai [1], Kazuki Matsui [1], Haruyo Kawaguchi, Tomomi Yamashita, Tomomi Mohri, Yasushi Fujio, Hiroyuki Nakayama *

Laboratory of Clinical Science and Biomedicine, Graduate School of Pharmaceutical Sciences, Osaka University, Osaka, Japan

ARTICLE INFO

Article history:
Received 27 June 2013
Available online 15 July 2013

Keywords:
CAMP
Myocarditis
Fibrosis
Cardiac fibroblast
P2X7 purinergic receptor

ABSTRACT

Fibrosis is one of the most common pathological alterations in heart failure, and fibroblast migration is an essential process in the development of cardiac fibrosis. Experimental autoimmune myocarditis (EAM) is a model of inflammatory heart disease characterized by inflammatory cell infiltration followed by healing without residual fibrosis. However, the precise mechanisms mediating termination of inflammation and nonfibrotic healing remain to be elucidated. Microarray analysis of hearts from model mice at multiple time points after EAM induction identified several secreted proteins upregulated during nonfibrotic healing, including the anti-inflammatory cathelicidin antimicrobial peptide (CAMP). Treatment with LL-37, a human homolog of CAMP, activated MAP kinases in fibroblasts but not in cardiomyocytes, indicating that fibroblasts were the target of CAMP activity. In addition, LL-37 decreased fibroblast migration in the in vitro scratch assay. P2X7 receptor (P2X7R), a well-known receptor for LL-37, was involved in LL-37 mediated biological effect on cardiac fibroblasts. Stimulation of BzATP, a P2X7R agonist, activated MAPK in fibroblasts, whereas the P2X7R antagonist, BBG, as well as P2X7R deletion abolished both LL-37-mediated MAPK activation and LL-37-induced reduction in fibroblast migration. These results strongly suggest that CAMP upregulation during myocarditis prevents myocardial fibrosis by restricting fibroblast migration via activation of the P2X7R–MAPK signaling pathway.

1. Introduction

Cardiovascular diseases, including myocardial infarction, hypertension, valvular insufficiency, and cardiomyopathies, are the primary causes of mortality in the Western world [1–3]. One of the major determinants of patient outcome is left ventricular (LV) remodeling, a chronic maladaptive process characterized by progressive ventricular dilation, myocardial hypertrophy, fibrosis, and ultimate deterioration of cardiac performance [4]. Cardiac fibroblasts are the most prevalent resident non-myocytes in the heart and migration of cardiac fibroblasts is closely associated with fibrosis which is a major determinant in ventricular remodeling after myocardial infarction, pressure overload, and myocarditis [5,6]. Prevention of excessive fibrosis is critical for ameliorating adverse cardiac remodeling. However the underlying molecular mechanism in regulation of cardiac fibroblast activation is not completely understood.

Inflammation is strongly involved in cardiac remodeling [7–9]. Cardiac damage or stress triggers infiltration of inflammatory cells, such as T cells, granulocytes, monocytes, and mast cells. Release of cytokines, growth factors, and chemokines by these infiltrating cells both exacerbates the disruption of myocardial structure and promotes tissue fibrosis [10–12]. Resolution of the inflammatory response and suppression of fibroblast activation may facilitate optimal cardiac adaptation after myocardial infarction or myocarditis, highlighting the potential of inhibitors of inflammation and fibroblast activation as therapeutics to prevent cardiac remodeling.

Experimental autoimmune myocarditis (EAM) is a rodent model of myocardial inflammation after viral infection. Immunization of BALB/c mice with myosin peptide leads to the infiltration of inflammatory cells, followed by spontaneous termination of the inflammatory response within 5 weeks and complete, nonfibrotic restoration of myocardial function [13,14]. While the role of proinflammatory cytokines and chemokines in EAM pathogenesis has been investigated extensively [15], little is known about the mechanism mediating recovery from inflammation without residual fibrosis.

In the present study, we investigated negative regulators of cardiac fibroblast activation in the EAM model by determining the genes upregulated during inflammatory phase of EAM using

* Corresponding author. Address: 1-6 Yamadaoka, Suita, Osaka 565-0871, Japan. Fax: +81 6 6879 8253.
E-mail address: nakayama@phs.osaka-u.ac.jp (H. Nakayama).
[1] These authors equally contributed to this work.

0006-291X/$ - see front matter © 2013 Published by Elsevier Inc.
http://dx.doi.org/10.1016/j.bbrc.2013.07.010

microarrays, real-time quantitative reverse transcription PCR (RT-PCR), and immunocytochemistry. Cathelicidin antimicrobial peptide (CAMP) exhibited one of the largest increases in expression during the inflammatory phase and upregulation was maintained during the recovery phase. CAMP and its human homolog LL-37 are cationic antimicrobial peptides [16], secreted by neutrophils and macrophages [17]. In addition to antimicrobial properties, CAMP/LL-37 suppresses the inflammatory response and promotes both angiogenesis and epithelial tissue repair [18–20]. We investigated the effect of LL-37 on cardiac fibroblast morphology, proliferation, and migration to assess possible functions in non-fibrotic adaptive remodeling. Our results demonstrate that CAMP/LL-37 negatively regulates migration of cardiac fibroblasts by activating P2X7 purinergic receptor (P2X7R) signaling.

2. Materials and methods

2.1. Antibodies and reagents

Primary antibodies against vimentin, CAMP, p38, and FAK were obtained from Santa Cruz Biotechnologies (Santa Cruz, CA), and antibodies against ERK, phospho-ERK1/2, JNK, phospho-JNK, and phospho-p38 were obtained from Cell Signaling Technology (Danvers, MA). BzATP and Brilliant Blue G (BBG) were obtained from Sigma–Aldrich (St. Louis, MO), and LL-37 was obtained from AnaSpec Inc. (Fremont, CA). P2X7 receptor null mice were obtained from the Jackson Laboratory (Bar Harbor, ME).

2.2. Generation of a murine EAM model

EAM was induced as previously described [13]. In brief, 6–8-weeks-old male BALB/c mice were immunized twice by subcutaneous administration of 100 μg peptides derived from amino acid sequence of the murine myosin heavy chain (MyHC-$\alpha_{614-634}$; Ac-SLKLMATLFSTYASAD-OH) in combination with an equal amount of the adjuvant complete H37 Ra (DIFCO). Hearts were harvested at the indicated times after EAM induction. All animal experiments were performed in compliance with Osaka University animal care guidelines and conformed to the Guide for the Care and Use of Laboratory Animals published by the US National Institute of Health (NIH publication No. 85-23, revised 1996).

2.3. Histological analysis and immunostaining

Hearts were harvested, rinsed, frozen in O.C.T. Compound (SAKURA Corp., Japan). Frozen sections of 5-μm thickness were prepared and fixed in 4% paraformaldehyde, permeabilized in 0.1% Triton X-100/PBS, and blocked with 3% bovine serum albumin (BSA). Some sections were incubated overnight at 4 °C in primary antibodies (anti-vimentin, 1:100 or control rabbit IgG, 1:100). After washing, a secondary antibody conjugated with Alexa Fluor-488 (Molecular Probes, Carlsbad, CA) was applied for 30 min at room temperature. Hoechst 33258 (Sigma–Aldrich) was used for staining nuclei. For CAMP immunostaining, the frozen heart sections were fixed in 4% paraformaldehyde for 15 min, permeabilized in 0.1% Triton X-100/PBS, and immersed in methanol containing 0.3% H_2O_2 to block intrinsic peroxidase activity. Sections were blocked with 1.7% rabbit serum/0.1% Triton X-100/Tris-buffered saline (TBS) and incubated overnight at 4 °C with primary antibodies anti-CAMP (1:100) or control goat IgG (1:100). Immunolabeling was visualized using the Vectastain ABC kit (VECTOR LABORATORIES, Burlingame, CA) following the manufacture's protocol. In brief, sections were incubated in ABC complex reagent, washed in 0.1% Triton X-100/TBS, and incubated in DAB substrate. Immunostained sections were examined under a light microscope (Olympus IXY70, Japan) equipped with epifluorescent optics.

2.4. Real-time quantitative RT-PCR

Total RNA was extracted from ventricular cells using QIAzol reagent (QIAGEN, Germantown, MD) following the manufacture's protocol. First strand cDNAs were synthesized from total RNA (1 μg) using ReverTra Ace (TOYOBO, Japan) and the oligo (dT) first strand primer. After cDNA synthesis, gene expression levels were estimated by real-time quantitative RT-PCR using the SYBR Green kit (Applied Biosystems, Carlsbad, CA). Sequences of gene-specific primers for real-time quantitative RT-PCR are shown in Supplementary Table S1.

2.5. Isolation and culture of rat neonatal cardiomyocytes and fibroblasts

Primary neonatal rat cardiomyocytes and fibroblasts were isolated as previously described [21]. In brief, hearts were excised, minced, digested with a solution containing 0.1% trypsin and 0.1% collagenase type IV to obtain a single-cell suspension, and separated into cardiomyocyte and non-myocyte fractions by differential adhesion. Isolated cardiomyocytes were cultured in Dulbecco's modified Eagles medium/Ham's F12 (ICN Biomedicals, Irvine, CA) supplemented with 5% fetal calf serum (FCS) and 0.1 mg/mL bromodeoxyuridine (to inhibit non-myocyte growth) at 37 °C in 95% air/5% CO_2 atmosphere. The non-myocyte fraction

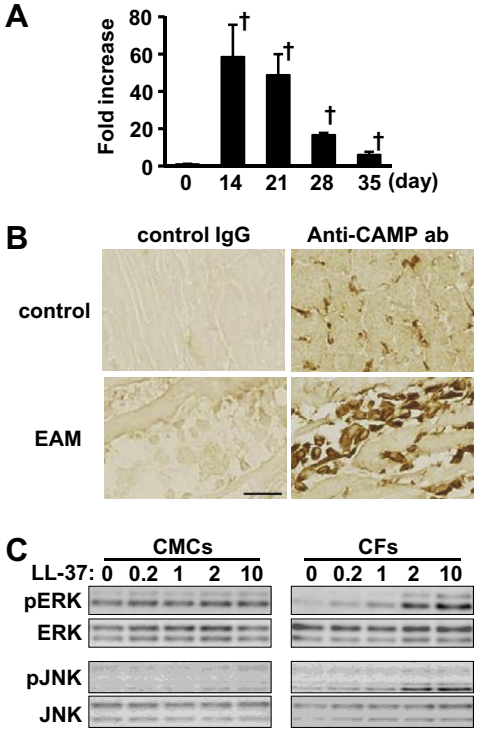

Fig. 1. Upregulation of CAMP expression in EAM model hearts and CAMP-induced phospho-activation of the MAP kinases, ERK, and JNK in cardiac fibroblasts. (A) The expression of CAMP was assessed by real-time quantitative RT-PCR at the indicated time points after EAM induction. The results were normalized to control hearts and are presented as mean ± S.D. (n = 3–6), $^{\dagger}P < 0.05$ vs. control. (B) Immunostaining with anti-CAMP antibody or normal goat IgG in sections obtained from control or EAM hearts at day 21 post-induction. Representative images are shown. (C) Cardiomyocytes (CMCs) and cardiac fibroblasts (CFs) were stimulated with LL-37 for 15 min at the indicated doses (μg/ml), and changes in protein expression were probed by Western blots using the indicated antibodies.

that primarily comprised of cardiac fibroblasts was grown to confluence in DMEM/F12 plus 5% FCS. To avoid contamination by myocytes, cardiac fibroblasts were used for experiments at passage 3. Primary neonatal mouse fibroblasts were isolated by the same procedure used for the preparation of neonatal rat fibroblasts.

2.6. Western blot analysis

For immunoblot analysis, cells were incubated for 12 h in serum-free medium, washed in cold PBS, and scraped into SDS sample buffer (62.5 mM Tris–HCl; pH 6.8, 10% glycerol, 2% SDS, 5% 2-mercaptoethanol, 0.001% bromophenol blue). Equal amounts of protein lysates were separated by SDS–PAGE on polyacrylamide gels and transferred to polyvinylidene difluoride membranes (Millipore, Bedford, MA). Membranes were blocked in TBS containing Tween (0.1%) and 2% nonfat dry milk for 1 h, followed by incubation with primary antibodies overnight at 4 °C. Bound antibodies were visualized using horseradish peroxidase (HRP)-conjugated secondary antibodies (Santa Cruz Biotechnology) and ECL reagent (Promega, Madison, WI). Band densities were measured by ImageQuant LAS 4010 using ImageQuant TL software (GE Healthcare, United Kingdom).

2.7. In vitro scratch assay

Migration of cardiac fibroblasts was assessed using an in vitro scratch assay following a previously described protocol [22]. In brief, cells were seeded and cultured in growth medium for 3 days, by which time cells reached 100% confluence. Confluent cultures were incubated for 8 h in serum-free medium and then scratched using a sterile pipette tip. Scratched cultures were treated with LL-37 alone or LL-37 plus a P2X7R antagonist (BBG) and photographed under a phase-contrast microscope at 0, 12, and 18 h. Migration of cells was estimated by measuring the width of the scratched area at each time point and the number of cells in the scratched area (cell-free at 0 h). Each assay was performed in triplicate in a blinded manner.

2.8. Immunocytochemistry

Immunocytochemistry of cultured cardiac fibroblasts was performed as described previously [23]. In briefly, fibroblasts were cultured on glass coverslips in serum-free medium containing LL-37 or LL-37 + BBG for 24 h, washed twice with PBS, fixed with 3.7% paraformaldehyde for 15 min, and permeabilized in 0.1% Triton X-100/PBS. An anti-focal adhesion kinase (FAK) antibody dissolved in 0.2% Triton X-100/PBS containing 3% BSA was applied for 1 h. After washing, an Alexa Fluor 488-conjugated secondary antibody or Alexa Fluor 546 phalloidin in 0.2% Triton X-100/PBS 1% BSA was applied for 30 min at room temperature. Immunofluorescence images were analyzed as described above. Ratio of cell length-to-width was assessed from images of phalloidin-stained cells.

2.9. Statistical analysis

All data are expressed as means ± S.D. or mean ± S.E. Statistically significant differences between experimental groups were determined using Student's *t*-test or one-way ANOVA, and $P < 0.05$ was considered statistically significant.

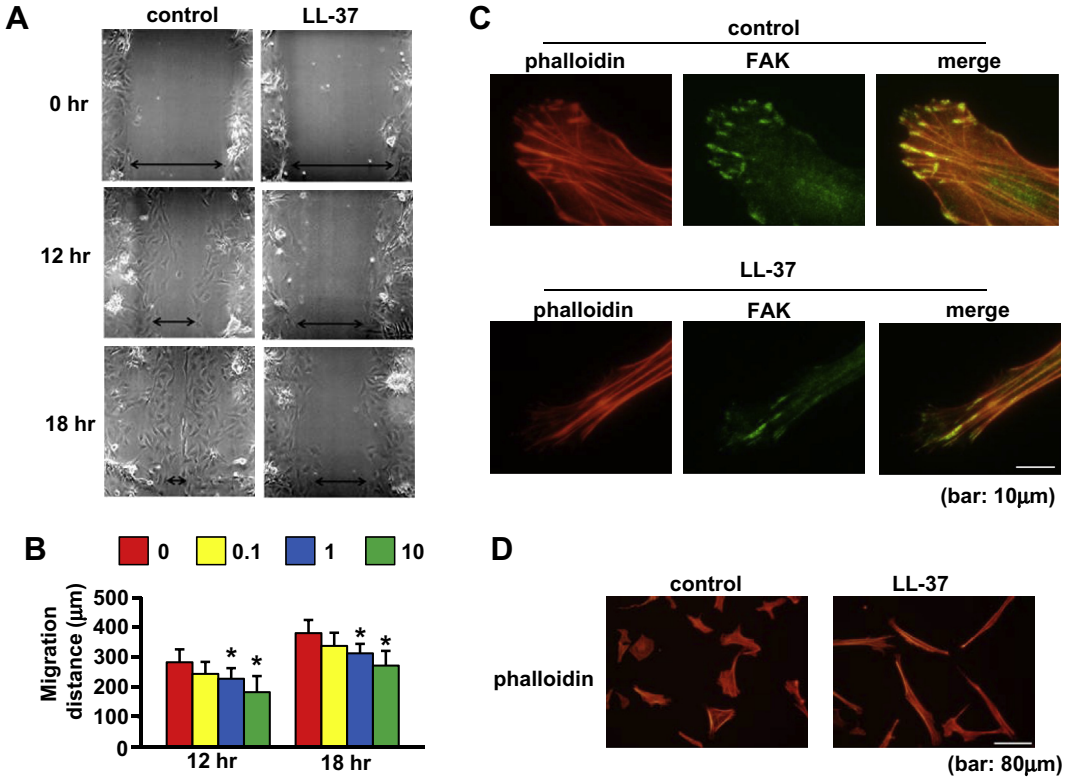

Fig. 2. LL-37 inhibited the migration of CFs, altered CF morphology, and reduced focal adhesion kinase (FAK). (A) Scratch assay of cell migration showing representative images of scratched confluent CF cultures maintained in the absence or presence of LL-37 (10 μg/ml) at 0, 12, and 18 h after scratch wounding. Arrows define the width of the scratched area in the CF monolayer. (B) Migration distance at 12 and 18 h after scratching. Data are expressed mean ± S.D. ($n = 6–7$), $^*P < 0.05$ vs. 0 μg/ml LL-37. (C) Representative fluorescent images of CFs immunostained for focal adhesion kinase (FAK, green) or phalloidin (red) 24 h after LL-37 stimulation. LL-37 suppressed FAK-actin colocalization. (D) Representative images showing changes in CF morphology in response to LL-37 (10 μg/ml) for 24 h.

3. Results

In a previous study, we measured the time course of inflammatory cell infiltration in mouse heart after induction of EAM and determined that peak inflammation occurred at 21 days post-immunization [14]. To trace the dynamics of cardiac fibroblasts in the EAM heart, frozen heart sections were prepared at various time points after EAM induction and activation of cardiac fibroblasts was assessed by vimentin immunostaining (Supplementary Fig. S1).

The mean number of cells immunopositive for the fibroblast marker vimentin peaked at day 21 and then decreased significantly (Supplementary Fig. S1A and B). Consistent with the activation of fibroblasts as revealed by vimentin, the expression levels of collagen 1, collagen 3, and fibronectin also peaked on day 21 and declined significantly thereafter (Supplementary Fig. S1C). These results suggest that the excessive activation of cardiac fibroblasts after induction of EAM was suppressed during the recovery phase.

To explore the mechanism underlying suppression of cardiac fibroblast activation during the recovery phase from EAM, we performed microarray analysis of mRNAs obtained from control and EAM hearts at day 21. From microarray results, we selected 13 upregulated genes encoding secreted proteins and assessed their individual roles in tissue repair according to previous reports (Supplementary Table S2). Among these upregulated genes, we focused on cathelicidin antimicrobial peptide (CAMP), which is a cationic antimicrobial peptide secreted by neutrophils and macrophages along with having anti-inflammatory and antimicrobial effects. The upregulation of CAMP was significantly observed using real-time quantitative RT-PCR on days 28 and 35 after EAM induction, suggesting the possibility that CAMP is associated with suppression of cardiac fibroblast activation during recovery phase (Fig. 1A). Immunohistochemistry from EAM and control hearts revealed that CAMP was predominantly expressed in infiltrating cells (Fig. 1B).

CAMP was previously reported to elicit various physiological functions on target cells via mitogen-activated protein (MAP) kinase pathways [24]. To define the target cells of secreted CAMP during EAM, we analyzed MAPK phosphorylation in cardiomyocytes and fibroblasts prepared from neonatal rat ventricles following stimulation with the human CAMP homolog, LL-37. In cardiomyocytes, MAPK family kinases ERK, JNK, and p38 were not activated by LL-37 as indicated by no change in phosphorylation status, whereas LL-37 dose-dependently increased ERK, JNK, and p38 phosphorylation in cultured cardiac fibroblasts (Fig. 1C, Supplementary Fig. S2).

We further examined the effect of LL-37 on cardiac fibroblast migration in an in vitro scratch assay. Compared with untreated control cultures, the scratch wound was wider with fewer migrating cells at 12 and 18 h after treatment with LL-37 (Fig. 2A). Estimation of fibroblast migration distance (Fig. 2B) indicated that LL-37 significantly and dose-dependently decreased the migration capacity of fibroblasts. As focal adhesion is closely related to cell migration, we analyzed the involvement of focal adhesion kinase (FAK) in LL-37 mediated cardiac fibroblast alteration. Immunocytochemistry for cardiac fibroblasts revealed that FAK localization partially disappeared on LL-37 stimulation (Fig. 2C). Incubation in LL-37 caused fibroblast elongation and significantly increased the length-to-width ratio of cells 24 h after stimulation (Fig. 2D). In contrast, LL-37 did not alter fibroblast proliferation as assessed by MTS assay (data not shown).

P2X7 purinergic receptor is a known LL-37 receptor, so we tested if the suppression of fibroblast migration was mediated by P2X7R–MAPK signaling pathways. The P2X7R agonist, BzATP, enhanced phosphorylation of ERK and JNK in a dose-dependent manner (Fig. 3A, Supplementary Fig. S3A), whereas the P2X7R antagonist BBG abolished LL-37-induced phosphorylation of ERK and JNK (Fig. 3B, Supplementary Fig. S3B), LL-37-induced fibroblast elongation (Fig. 3C and D), and LL-37-induced suppression of fibroblast migration in the scratch assay (Fig. 3E).

To further corroborate the involvement of P2X7R–MAPK signaling pathways, we examined migration of fibroblasts isolated from the heart of P2X7R null mice and control. Consistent with previous results, LL-37-induced suppression of migration (Fig. 4A and B) and LL-37-induced phosphorylation of ERK and JNK were significantly attenuated in P2X7R deficient cardiac fibroblasts (Fig. 4C, Supplementary Fig. S4). Moreover, LL-37-induced fibroblast elongation was abrogated by P2X7R deletion (Fig. 4D).

4. Discussion

In the present study, we have demonstrated for the first time that CAMP is significantly upregulated in the heart during the inflammatory and recovery phases of murine experimental autoimmune myocarditis and that CAMP regulates fibroblast activation and migration by activating P2X7R–MAPK signaling pathways. These results suggest CAMP as a potential molecular target for therapies to prevent cardiac fibrosis in ventricular remodeling caused by cardiac inflammation.

One of the most important features of the EAM model is spontaneous recovery without histological vestige. There are compel-

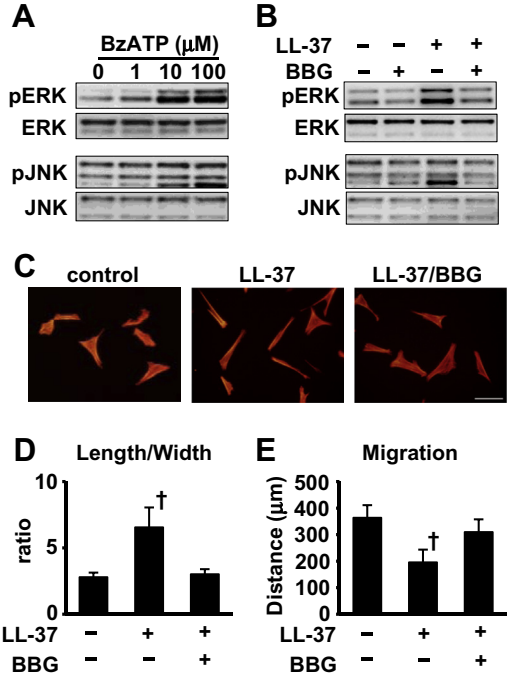

Fig. 3. The effects of LL-37 on CFs are dependent of P2X7 receptor signaling. (A) Phosphorylation of ERK and JNK in cultured CFs after 15 min of stimulation by the P2X7R agonist BzATP at the indicated concentrations. (B) Inhibition of LL-37-induced phosphorylation of ERK and JNK by the P2X7 antagonist BBG (10 μM). LL-37 was applied at 10 μg/ml for 15 min after 1 h pretreatment with BBG. (C) Inhibition of LL-37-induced changes in CF morphology by BBG (10 μM). LL-37 (10 μg/ml) was applied alone for 24 h (middle panel) or together with BBG (right panel). (D) Inhibition of the LL-37-induced increase in CF length-to-width ratio by BBG. Drugs applied same as in (C). Fifty cells from 3 cultures measured for each group. (E) Reversal of the LL-37-mediated suppression of CF migration by BBG. Migration distance 18 h after monolayer scratch was assessed with or without LL-37 in the presence or absence of BBG. Data are expressed as mean ± S.D. ($n = 10$ cultures for each experiment). $^{\dagger}P < 0.05$ vs. other treatment groups.

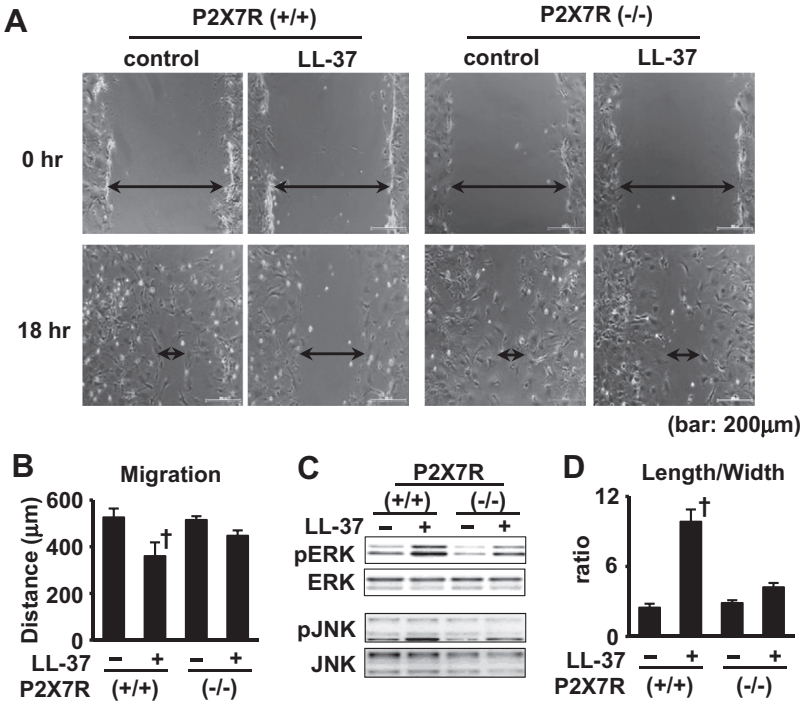

Fig. 4. The effects of LL-37 on CFs are abrogated by P2X7 receptor (P2X7R) deletion. (A) Scratch assay of cell migration showing representative images of scratched confluent CF cultures isolated from control (P2X7R +/+) or P2X7R deficient (P2X7R −/−) mice maintained in the absence or presence of LL-37 (10 μg/ml) at 0, and 18 h after scratch wounding. (B) Reversal of the LL-37-mediated suppression of migration in P2X7R deficient CF. Migration distance 18 h after monolayer scratch was assessed with or without LL-37 (10 μg/ml) for P2X7R deficient or control fibroblasts. Data are expressed as mean ± S.D. ($n = 4$ cultures for each experiment). (C) Phosphorylation of ERK and JNK in cultured CFs isolated from control or P2X7R deficient mice after 15 min of stimulation by LL-37 (10 μg/ml). (D) Abrogation of the LL-37-induced increase of length-to-width ratio in P2X7R deficient CFs after 24 h stimulation of LL-37 (10 μg/ml). Fifty cells measured from 3 cultures for each group. $^{\dagger}P < 0.05$ vs. other groups.

ling evidence that inflammation and resolution in the EAM model are mediated by distinct sets of cytokines: Th1 (IL-2 and IFN-γ), Th17 (IL-17 and IL-23), and other proinflammatory cytokines (IL-1 and TNFα) have been detected only in the inflammatory phase, whereas the production of Th2 cytokines such as IL-10 have been detected only during the recovery phase [14,25]. A recent report suggested that the MyD 88−IL-1 signaling pathway in fibroblasts is crucial for the transition from inflammation to fibrosis [26]. Our results suggest that CAMP can block this transition and instead promote nonfibrotic recovery.

Cardiomyocytes and fibroblasts in vivo are likely exposed to CAMP secreted from infiltrating cells, but CAMP activated MAPK signaling only in fibroblasts. We observed no effect of the human CAMP homolog LL-37 on cardiomyocyte MAPK activation, survival, hypertrophy, or expression of cytokines (data not shown). CAMP is a cationic antimicrobial peptide secreted by neutrophils and macrophages, which elicits a multitude of physiological responses, including suppression of inflammation [19] and promotion of angiogenesis [20]. In contrast to the anti-inflammatory effect in mouse heart, CAMP may be proinflammatory in other tissues or physiological contexts. In a recent report, neutrophil-derived CAMP induced recruitment of activated monocytes and promoted atherosclerosis in CAMP-null mice that also lacked Apolipoprotein E [27]. Hence, the role of CAMP in inflammation appears to depend on the cellular environment of target cells. However, inconsistent effects of CAMP/LL-37 on fibroblasts have also been reported. Oudhoff et al. [28] reported that CAMP actually enhanced fibroblast migration within a narrow concentration range [28], whereas in our study, LL-37 clearly suppressed cardiac fibroblast migration at all concentrations. In addition, we found no enhancement of fibroblast proliferation by LL-37, in contrast to Oudhoff et al. [28]. Administration of LL-37 suppressed collagen synthesis in dermal fibroblasts [24,29], consistent with the antifibrotic role of LL-37 in cardiac inflammation. Intriguingly, both type 1 and 3 collagen expression levels fell dramatically at around the time that LL-37 expression peaked. While elucidation of the MAPK-dependent pathways that suppress CF migration requires further study, we also demonstrated that stimulation by LL-37 altered FAK localization in cardiac fibroblast, suggesting that restrained focal adhesion is involved in underlying mechanism of CAMP-mediated suppression of migration.

CAMP is known to activate receptors and intracellular signaling cascades in addition to P2X7 and MAPKs. For instance, CAMP stimulation activated the STAT3 pathway via EGFR in keratinocyte [30] and PI3K via EGFR in corneal epithelial cells [31]. In intestinal epithelial cells, like cardiac fibroblasts, CAMP activates MAP kinases [24,32]. We did assess whether Akt and/or PI3K pathways were evoked by CAMP in cardiac fibroblasts but observed no activation. Similarly, we examined the involvement of EGFR and FPRL-1 in CAMP-mediated MAPK activation and found no effect of EGFR and FPRL-1 antagonists (data not shown). Hence, the downstream signaling events induced by CAMP appear to be mediated, at least partially, by P2X7R in rat cardiac fibroblasts. Whether P2X7R−MAPK signaling is a ubiquitous pathway regulating fibroblast activation and migration in other tissues is still unclear. In human fibroblast cell lines, however, silencing of P2X7R had little effect on ATP-mediated migration [33]. This question is of paramount importance given that numerous diseases are associated with fibrosis.

In conclusion, the present study revealed that CAMP is upregulated during both the inflammatory and recovery stages of EAM. Administration of CAMP suppressed cardiac fibroblast migration via P2X7R. We suggest that CAMP is a novel candidate treatment for prevention of fibrosis following cardiac inflammation.

Acknowledgments

We thank Wakako Okamoto for her excellent secretarial work. The present study was supported by a Grant-in-Aid for Scientific Research from the Ministry of Education, Culture, Sports, Science and Technology in Japan and in part by a research grant from the Suzuken Memorial Foundation.

Appendix A. Supplementary data

Supplementary data associated with this article can be found, in the online version, at http://dx.doi.org/10.1016/j.bbrc.2013.07.010.

References

[1] A. Qaseem, S.D. Fihn, P. Dallas, et al., Management of stable ischemic heart disease: summary of a clinical practice guideline from the American College of Physicians/American College of Cardiology Foundation/American Heart Association/American Association for Thoracic Surgery/Preventive Cardiovascular Nurses Association/Society of Thoracic Surgeons, Ann. Intern. Med. 157 (2012) 735–743.
[2] G.A. Mensah, D.W. Brown, An overview of cardiovascular disease burden in the United States, Health Aff. (Millwood) 26 (2007) 38–48.
[3] R.E. Hobbs, Guidelines for the diagnosis and management of heart failure, Am. J. Ther. 11 (2004) 467–472.
[4] M.A. Pfeffer, E. Braunwald, Ventricular remodeling after myocardial infarction. Experimental observations and clinical implications, Circulation 81 (1990) 1161–1172.
[5] A.M. Segura, O.H. Frazier, L.M. Buja, Fibrosis and heart failure, Heart Fail. Rev. (2012).
[6] E.M. Zeisberg, R. Kalluri, Origins of cardiac fibroblasts, Circ. Res. 107 (2010) 1304–1312.
[7] D. Carnevale, G. Cifelli, G. Mascio, et al., Placental growth factor regulates cardiac inflammation through the tissue inhibitor of metalloproteinases-3/tumor necrosis factor-alpha-converting enzyme axis: crucial role for adaptive cardiac remodeling during cardiac pressure overload, Circulation 124 (2011) 1337–1350.
[8] N.G. Frangogiannis, Regulation of the inflammatory response in cardiac repair, Circ. Res. 110 (2012) 159–173.
[9] D.L. Mann, The emerging role of innate immunity in the heart and vascular system: for whom the cell tolls, Circ. Res. 108 (2011) 1133–1145.
[10] N.G. Frangogiannis, Chemokines in the ischemic myocardium: from inflammation to fibrosis, Inflamm. Res. 53 (2004) 585–595.
[11] M. Bujak, N.G. Frangogiannis, The role of tgf-beta signaling in myocardial infarction and cardiac remodeling, Cardiovasc. Res. 74 (2007) 184–195.
[12] A. Valaperti, R.R. Marty, G. Kania, et al., Cd11b+ monocytes abrogate th17 cd4+ t cell-mediated experimental autoimmune myocarditis, J. Immunol. 180 (2008) 2686–2695.
[13] N. Neu, N.R. Rose, K.W. Beisel, et al., Cardiac myosin induces myocarditis in genetically predisposed mice, J. Immunol. 139 (1987) 3630–3636.
[14] T. Yamashita, T. Iwakura, K. Matsui, et al., Il-6-mediated th17 differentiation through rorgammat is essential for the initiation of experimental autoimmune myocarditis, Cardiovasc. Res. 91 (2011) 640–648.
[15] J. Suzuki, M. Ogawa, R. Watanabe, et al., Autoimmune giant cell myocarditis: clinical characteristics, experimental models and future treatments, Expert Opin. Ther. Targets 15 (2011) 1163–1172.
[16] M.F. Burton, P.G. Steel, The chemistry and biology of ll-37, Nat. Prod. Rep. 26 (2009) 1572–1584.
[17] B. Agerberth, J. Charo, J. Werr, et al., The human antimicrobial and chemotactic peptides ll-37 and alpha-defensins are expressed by specific lymphocyte and monocyte populations, Blood 96 (2000) 3086–3093.
[18] K.A. Henzler Wildman, D.K. Lee, A. Ramamoorthy, Mechanism of lipid bilayer disruption by the human antimicrobial peptide, ll-37, Biochemistry 42 (2003) 6545–6558.
[19] N. Mookherjee, K.L. Brown, D.M. Bowdish, et al., Modulation of the tlr-mediated inflammatory response by the endogenous human host defense peptide ll-37, J. Immunol. 176 (2006) 2455–2464.
[20] R. Koczulla, G. von Degenfeld, C. Kupatt, et al., An angiogenic role for the human peptide antibiotic ll-37/hcap-18, J. Clin. Invest. 111 (2003) 1665–1672.
[21] K. Yamauchi-Takihara, Y. Ihara, A. Ogata, et al., Hypoxic stress induces cardiac myocyte-derived interleukin-6, Circulation 91 (1995) 1520–1524.
[22] C.C. Liang, A.Y. Park, J.L. Guan, In vitro scratch assay: a convenient and inexpensive method for analysis of cell migration in vitro, Nat. Protoc. 2 (2007) 329–333.
[23] A.M. Manso, S.M. Kang, S.V. Plotnikov, et al., Cardiac fibroblasts require focal adhesion kinase for normal proliferation and migration, Am. J. Physiol. Heart Circ. Physiol. 296 (2009) H627–H638.
[24] H.J. Park, D.H. Cho, H.J. Kim, et al., Collagen synthesis is suppressed in dermal fibroblasts by the human antimicrobial peptide ll-37, J. Invest. Dermatol. 129 (2009) 843–850.
[25] Y. Okura, T. Yamamoto, S. Goto, et al., Characterization of cytokine and inos mrna expression in situ during the course of experimental autoimmune myocarditis in rats, J. Mol. Cell. Cardiol. 29 (1997) 491–502.
[26] P. Blyszczuk, G. Kania, T. Dieterle, et al., Myeloid differentiation factor-88/interleukin-1 signaling controls cardiac fibrosis and heart failure progression in inflammatory dilated cardiomyopathy, Circ. Res. 105 (2009) 912–920.
[27] Y. Doring, M. Drechsler, S. Wantha, et al., Lack of neutrophil-derived cramp reduces atherosclerosis in mice, Circ. Res. 110 (2012) 1052–1056.
[28] M.J. Oudhoff, M.E. Blaauboer, K. Nazmi, et al., The role of salivary histatin and the human cathelicidin ll-37 in wound healing and innate immunity, Biol. Chem. 391 (2010) 541–548.
[29] H.J. Park, S.M. Ock, H.J. Kim, et al., Vitamin C attenuates ERK signalling to inhibit the regulation of collagen production by ll-37 in human dermal fibroblasts, Exp. Dermatol. 19 (2010) e258–e264.
[30] S. Tokumaru, K. Sayama, Y. Shirakata, et al., Induction of keratinocyte migration via transactivation of the epidermal growth factor receptor by the antimicrobial peptide ll-37, J. Immunol. 175 (2005) 4662–4668.
[31] J. Yin, F.S. Yu, Ll-37 via EGFR transactivation to promote high glucose-attenuated epithelial wound healing in organ-cultured corneas, Invest. Ophthalmol. Vis. Sci. 51 (2010) 1891–1897.
[32] J.M. Otte, A.E. Zdebik, S. Brand, et al., Effects of the cathelicidin ll-37 on intestinal epithelial barrier integrity, Regul. Pept. 156 (2009) 104–117.
[33] J.B. Chen, W.J. Liu, H. Che, et al., Adenosine-5′-triphosphate up-regulates proliferation of human cardiac fibroblasts, Br. J. Pharmacol. 166 (2012) 1140–1150.